A Virtual Target Radar System for Small Arms Fire Training

Clive M. Alabaster[1], Evan J. Hughes[1] & Daniel Flores-Tapia[2]

[1] White Horse Radar Limited
Royal Wootton Bassett, UK
clive@whradar.com, evan@whradar.com

[2] Department of Physics and Astronomy
University of Manitoba
Winnipeg, Canada

***Abstract*—This paper describes the development of a novel radar system acting as a virtual target to assist in the training of a marksman. It provides the miss distance of a bullet from an aim point in two axes as the bullet passes through the target plane. Initial work indicates that a low-cost solution can achieve millimetre-level accuracy irrespective of projectile velocity over a wide range of environmental conditions.**

Keywords—CW radar, virtual target

I. INTRODUCTION

In the training of a marksman for small arms fire on a firing range, an aim point is traditionally presented on a paper target which also acts as a witness screen to record the mis-distance from the hole left by the passing bullet. Paper targets have to be replaced regularly and are cumbersome and time consuming to use, especially over long ranges. These have gradually become replaced by acoustic or optical sensor systems which can automatically log the mis-distance of each bullet and relay this information to the shooter. Acoustic sensors triangulate the position of a supersonic bullet using three acoustic sensors on the ground which receive the conical shock wave created by the round passing above them. They do not work accurately for the spherical shaped pressure wave arising from sub-sonic rounds and are prone to errors due to variations in the velocity of sound in air (e.g. due to temperature, density variations) and due to wind. This limits their use to indoor ranges [1]. Optical systems use multiple parallel light beams and optical sensors arranged in a grid around a frame. As the round passes through the frame one or more of the light beams is cut and the position of the passing round is recorded. These can be expensive, do not cope well with changes in ambient light levels and are prone to damage from stray shots or debris kicked up by the fall of the shot beyond the target [2][3]. A low-cost solution has been sought which would overcome the problems of existing systems, operate in all conditions (indoors and outside) for all bullet velocities and yet yield an accuracy of about 4mm which is approximately half the calibre of a standard NATO round of 7.62mm as a design goal. Radar boasts good all-weather and motion detection capabilities, however, the range accuracy requirement of a fraction of a wavelength for typical centimetric wave frequencies could clash with the low-cost expectation. Nevertheless, the modest cost of commercially available radar hardware and processing power makes a radar based solution a viable option.

A prototype system has been designed initially under a knowledge transfer partnership (a UK government initiative to support a UK industrial partner in a project which requires the expertise and collaboration of a UK university); the concept was originally reported in [2]. More recently, the system has been further developed into a working prototype virtual targeting radar (VTR).

Section II of this paper describes the concept of operation of the VTR system together with the theory of its design and signal processing. Parameters of its hardware design are presented in section III. In section IV, some simulation results and results of trial firings are presented and discussed together with analysis on the accuracy of the system. A few conclusions are drawn in section V and proposed further work is described.

II. CONCEPT AND THEORY OF OPERATION

A. The Concept of Operation

The VTR consists of two radars at ground level separated by a baseline distance, d, which is approximately 2 metres. Each radar boresight is inclined upwards at 45º so that the boresights intersect at right angles. The region in which the beams overlap in the plane defined by the two boresight vectors defines the targeting plane, as shown in Fig. 1. The shooter is presented with an aim point by the intersection of two visible laser beams from a pair of diode lasers aligned to the boresight of each radar. A bullet passing through the beams between set velocity and amplitude limits triggers the recording of the data by each radar which is processed using inverse synthetic aperture radar (ISAR)-like techniques to extract the range to the bullet. Each radar measures the range to the bullet as it passes through the targeting plane. This yields the x and y coordinates of the bullet and hence its mis-distance in each plane from the target centre.

Each radar module uses a differential phase difference method between two carrier frequencies to measure the range to the bullet. If a bullet is shot along the axis of the range then it intersects the targeting plane at a right angle. As it transits the targeting plane its Doppler shift goes through zero Hertz (Hz);

the bullet range at this point is computed. Each radar emits two continuous wave (CW) tones in the I-band and which are separated by a spacing frequency Δf, typically of a few MHz. Returns from the bullet are phase shifted over the two-way path to the bullet and back. Since the two-way distance exceeds a wavelength the 2π phase wrapping introduces range ambiguity. This ambiguity is resolved using the second carrier frequency. Returns from each carrier are down-converted into separate receiver channels By comparing the phase shift over the two carriers one obtains a differential phase shift equivalent to a carrier frequency equal to Δf. Since Δf is in the HF band the two-way path length does not exceed a wavelength and so no range ambiguity exists. Thus the range is measured at the point of closest approach, i.e. the targeting plane. Once this range has been measured along two orthogonal axes one has the *x,y* coordinates at which the bullet intersected the targeting plane and hence the mis-distance from the aim point.

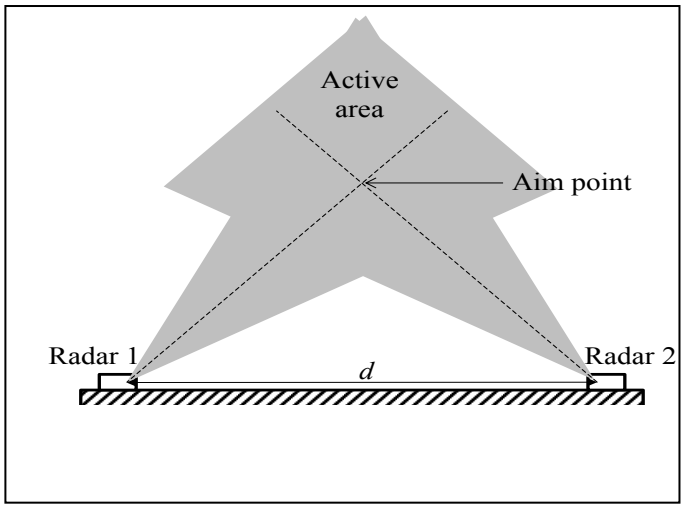

Figure 1. VTR System Geometry

The ability of the radar to make an accurate measurement of bullet range depends on the validity of the assumption that the bullet trajectory is orthogonal to the targeting plane and on the signal to noise ratio (SNR) of the returns. The differential phase method described here can achieve accuracies in the order of a fraction of a wavelength at I-band. It is worth noting that this radar system cannot resolve multiple targets. Whilst each radar can measure range very accurately, it has no range resolution whatsoever; returns from multiple scatterers would yield their vector sum and the system would declare one result which was not a true indication of any of the scatterers. Static clutter can be eliminated by applying a dc block on the video output signals. Since only one bullet would be expected to be within the beam at any one time, even for machine gun fire, this does not present a problem.

B. Theory of Operation

Each radar emits two CW tones; the frequencies of the two tones from one radar differ from those of the other in order to enable filtering to provide isolation between the two. It is sufficient for now to consider the operation of just one of the radars. The two frequencies are defined by a centre frequency, f_c, and a difference frequency, Δf. The upper and lower frequencies are therefore:

$$f_U = f_c + \Delta f/2 \tag{1a}$$

$$f_U = f_c - \Delta f/2 \tag{1b}$$

The choice of f_c was nominally 10GHz so that the length of a typical bullet corresponds to a half the free-space wavelength (λ = 3cm) and this coincidence maximizes the radar cross section (RCS) of the bullet. At the two frequencies, f_L and f_U we have two corresponding wavelengths, λ_L and λ_U, in which the suffix $_L$ denotes the lower frequency and the suffix $_U$ denotes the upper frequency. This gives rise to phase shifts, φ_L and φ_U over the range, R, to the bullet at any instant.

At f_L we have:

$$\varphi_L = \frac{4\pi R}{\lambda_L} = \frac{4\pi R f_L}{c} \tag{2a}$$

and at f_U we have:

$$\varphi_U = \frac{4\pi R}{\lambda_U} = \frac{4\pi R f_U}{c} \tag{2b}$$

where c is the speed of light.

The phase difference between the two channels is therefore:

$$\Delta\varphi = \varphi_U - \varphi_L = \frac{4\pi R(f_U - f_L)}{c} = \frac{4\pi R \Delta f}{c} \tag{3}$$

Due to the 2π phase wrapping, $\Delta\varphi$ should not exceed 2π otherwise range ambiguity results. For $\Delta\varphi = 2\pi$, $R = R_{mu}$, where R_{mu} is the maximum unambiguous range, i.e.

$$2\pi = \frac{4\pi R_{mu} \Delta f}{c} \tag{4}$$

which, on re-arranging gives:

$$\Delta f = \frac{c}{2R_{mu}} \tag{5}$$

and is a classic result for a stepped or dual frequency waveform.

The complex output voltages can therefore be written:

$$v_L = v_{QL} - j.v_{IL} \tag{6a}$$

and

$$v_U = v_{QU} - j.v_{IU} \tag{6b}$$

in which the suffixes I and Q denote the in-phase and quadrature phase channel outputs, respectively.

The complex baseband signals are processed by a Fourier Transform. This yields a power spectrum and an angle

spectrum. Let us denote the complex quadrature output signal previously given by the equation pair (6) in general as *v(t)*. The suffixes *L* and *U* can be re-introduced later, as necessary.

Substituting (2) into (6) gives:

$$v(t) = \cos\left(\frac{4\pi R}{\lambda}\right) - j\sin\left(\frac{4\pi R}{\lambda}\right) \tag{7a}$$

which may be re-cast in exponential form as

$$v(t) = e^{-j\frac{4\pi R}{\lambda}} \tag{7b}$$

The Fourier transform of this signal is defined as:

$$V(\omega) = F\{v(t)\} = \int_{-\infty}^{+\infty} v(t)e^{-j\omega t}dt \tag{8a}$$

v(t) is defined within limits of time from $t = 0$ to t_{int} , where t_{int} is the integration time, therefore the limits of integration may be reduced to this range

$$V(\omega) = \int_0^{t_{\text{int}}} v(t)e^{-j\omega t}dt \tag{8b}$$

V(ω) will be complex because the function *v(t)* is not an even function i.e. not symmetrical about $t = 0$ and so is comprised of sines and cosines.

The Fourier transform of the complex quadrature output signal is therefore given by

$$V(\omega) = \int_0^{t_{\text{int}}} e^{-j\frac{4\pi R(t)}{\lambda}} e^{-j\omega t}dt$$

Hence for the upper and lower frequencies we have:

$$V_U(\omega) = \int_0^{t_{\text{int}}} e^{-j\left(\omega_U t + \frac{4\pi R(t)}{\lambda_U}\right)} dt \tag{9a}$$

and

$$V_L(\omega) = \int_0^{t_{\text{int}}} e^{-j\left(\omega_L t + \frac{4\pi R(t)}{\lambda_L}\right)} dt \tag{9b}$$

in which *R(t)* is the range as a function of time.

Taking the phase spectrum of the difference between this equation pair one may derive *R(t)*.

$$R(t) \propto \angle\left[V_U(\omega) - V_L(\omega)\right] \tag{10}$$

Taking the phase difference at zero (or at a very low) Doppler frequency yields the range at the point of closest approach to the radar which corresponds to the targeting plane for a trajectory which is perpendicular to the targeting plane.

Consider the geometry of the situation depicted in Fig. 2. The targeting plane is defined in the *x,y* plane. One radar is placed at the origin (*0,0,0*) and the other radar is placed a distance *d* from the first along the *x*-axis, i.e. at coordinates of (*d,0,0*). The centre is the point at which the boresights of both radars intersect and since both are inclined at 45°, the target centre lies at coordinates (*d/2,d/2,0*). The bullet intersects the targeting plane at a right angle for a bullet trajectory which is parallel to the *z*-axis. Let the range to the bullet in the targeting plane as measured by radars 1 and 2 be R_1 and R_2 respectively. Contours of equal range are circles centred at the locations of the radars (strictly, the phase centres of the radar antennas). The two circles of radii R_1 and R_2 overlap at two points given by [4]:

$$x = \frac{d^2 - R_2^2 + R_1^2}{2d}, \qquad y = \sqrt{R_1^2 - x^2} \tag{11}$$

This yields two intercept points; one above the baseline (positive *y*), the other below the baseline (negative *y*). The latter case can be dismissed and the result can be taken as the former case. This intercept point must now be offset by the *x* and *y* coordinates of the aim point which are (*d/2*, *d/2*) and is the miss distance result declared to the shooter.

The I/Q Doppler outputs from the radar units are sampled with two 4-channel analogue-to-digital converters running at a 100kHz sample frequency. The radii R_1 and R_2 are calculated for 5 sample points before and after the zero Doppler point. The mean of each set of 11 values is taken to provide averaged values for the radii R_1 and R_2 and then the *x* and *y* positions are generated.

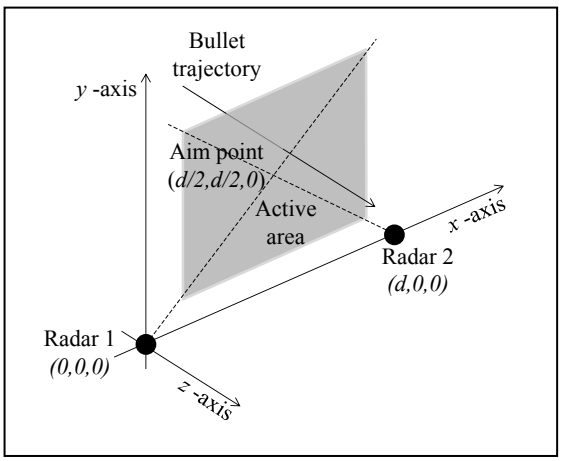

Figure 2. VTR Coordinate System

III. THE HARDWARE DESIGN

A. Radar Hardware

Radar returns are down-converted using a double superheterodyne receiver employing an image rejection mixer (IRM) in which the first local oscillator (LO1) runs at f_c and the system's first intermediate frequency (1st IF) is tuned to $\Delta f/2$. The IRM has two outputs; one sensitive to the upper sideband and the other sensitive to the lower sideband. In this way, returns at the two carrier frequencies fall in each other's image band and are separated into the two channels in the 1st IF. The IRM offers approximately 25 dB of channel isolation. After amplification and filtering, a second stage of down-conversion is conducted in each channel direct to baseband using quadrature detectors. This results in in-phase (I) and quadrature phase (Q) channel outputs. An RF low noise amplifier (LNA) is included on the front end in order to minimize the system

noise figure and maintain an adequate SNR at the receiver outputs. The receiver block diagram is shown at Fig. 3.

The two output signals are generated by mixing the LO1 and LO2 signals, as shown in Fig. 4. Whilst this is a simple arrangement there remains some breakthrough of the LO1 signal and intermodulation products on the output spectrum.

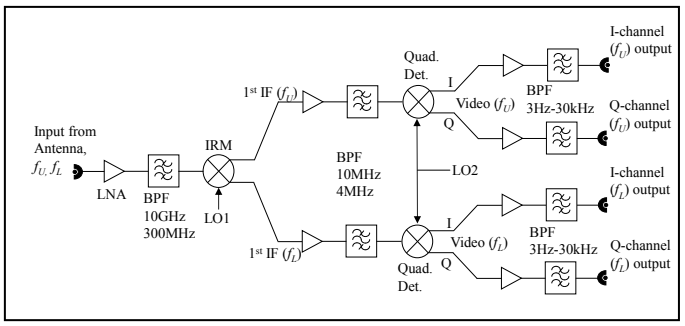

Figure 3. VTR Receiver Block Diagram

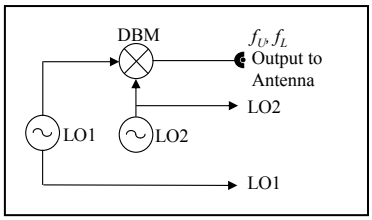

Figure 4. VTR Receiver

At present the antenna system employs a bistatic arrangement of two wide beam/low gain horn antennas. The antenna centres are approximately 10cm apart and the targeting plane is in line with the midway point between the two antennas. Although this bistatic approach reduces the coupling between receive and transmit as compared to that provided by a circulator, the level of isolation is not quite sufficient to suppress interference from spurious modulation products arising due to the transmissions from the opposite radar via a sidelobe to sidelobe path. To alleviate this problem the antennas forming the bistatic arrangement of both radars are set up to radiate a horizontally plane polarized signal and to receive vertically plane polarized signals, so providing an additional 20dB of isolation. While this suppresses the interference, the desired returns are also reduced due to the lower cross-polar RCS of bullets (section IIIB). Nevertheless, there is a net gain in signal to interference ratio which gives a workable system.

A summary of the radar parameters is provided in Table 1.

TABLE I. RADAR PARAMETERS

Parameter	Value
Carrier Frequencies (radar 1, 2)	9880, 9900, 10090, 10110 MHz
LO1 frequencies (radar 1, 2)	9890, 10100 MHz
Δf, (R_{mu})	20 MHz, (7.5 m)
Transmitter Power (CW)	+15 dBm per signal
Antenna Gain	10 dB*i*
1st IF centre frequency bandwidth	10 MHz ± 60kHz
Receiver Noise Figure	≤ 6 dB
P 1dB	≥ -25 dBm
Receiver Gain Gain balance Phase matching	60 dB nominal 0.5 dB 5 degrees
Image channel rejection	≥ 25 dB
IF Stop band rejection	≥ 60 dB at 10 MHz
Doppler bandwidth	3 Hz – 30 kHz

B. *Bullet Radar Detectability*

Earlier work [3] reported on the measurement of the RCS of a variety of bullets at 10GHz. A bullet of diameter = 7.62mm and length 28.4mm (close to one wavelength) has a peak H/H RCS when seen orthogonal to the axis of the bullet of 0.001 m^2 (the peak V/V RCS was measured at 0.0007 m^2 under the same conditions). It was found that the RCS of a bullet could be approximated by that of a metal cylinder of the same dimensions as those of the bullet.

The H/H target RCS of 0.001 m^2 at a range of 4 metres would yield a SNR of 53 dB (assuming a noise limited detection and the absence of any losses), or 51.5 dB for the V/V RCS case. Even allowing for further losses of 5dB for the cross-polar RCS of a smaller bullet, and the inclusion of 10 dB of additional losses, the SNR would be reduced to 36.5 dB.

IV. RESULTS AND DISCUSSION

A. *Simulated Waveforms*

The waveforms generated by a bullet passing a single radar have been simulated and are presented in Figs. 5-7. Fig. 5 presents the I and Q channel waveforms for one of the carrier frequencies transiting the beam in approximately 1.5 ms. Note the quadrature relationship between the two waveforms, the phase reversal at mid-way through the waveform as the bullet passes the targeting plane and the amplitude modulation due to the gain pattern of the antenna. Fig. 6 illustrates the power spectrum of the chirp waveform shown in Fig. 5 but with Gaussian noise added having a SNR of 20 dB. Fig. 7 depicts the differential phase spectrum between the two carriers; the upper plot giving the absolute phase difference and the lower plot showing the phase difference as it wraps between values of $\pm \pi$ radians.

B. *Measured Waveforms*

Data captured from a 7.62mm round passing through the target at 823 m/s is illustrated in Fig. 8. The data burst lasts for

approximately 1.8ms as the bullet transits the radar beam. The upper plot is the I and Q channel data at f_U and the lower plot shows the I and Q channel data at f_L. These waveforms resemble the simulated waveforms of Fig. 5 quite well. The system processes this data and declares the miss distance from the centre in both x and y coordinates. The peak SNR at the zero crossing point is approximately 37 dB, which is in close agreement to the value predicted in section IIIB.

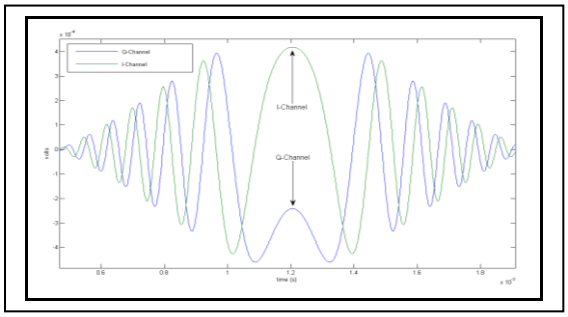

Figure 5. Simulated I & Q Waveforms [2]

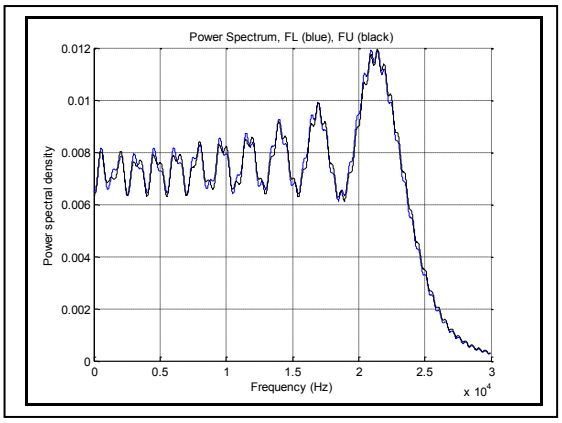

Figure 6. Simulated Power Spectrum, SNR = 20dB

C. *Analysis of Accuracy*

The current signal processing assumes that the bullet trajectory is parallel to the z –axis since this ensures that the targeting plane does coincide with the point of closest approach and hence of zero Doppler. If the actual bullet trajectory has a gradient in either the horizontal (x,z) or vertical (y,z) planes, then the radars measure a range to the point of closest approach which is too low and an incorrect result is declared. The magnitude of this error depends on the baseline separation between the radars, the trajectory gradient and the actual miss distance from the target centre at which the bullet passes the targeting plane. The worst case gradient arises for the shortest length of the range (the distance between shooter and target) and the maximum displacement of the shooter from the centre of the range (limited to half the width of the shooting lane).

For a range length of 25m and a displacement of 2m, the angle of the trajectory is 0.08 radians (4.6º). If the actual placement of the shot has zero x –axis miss distance then the declared result has a y-axis error only.

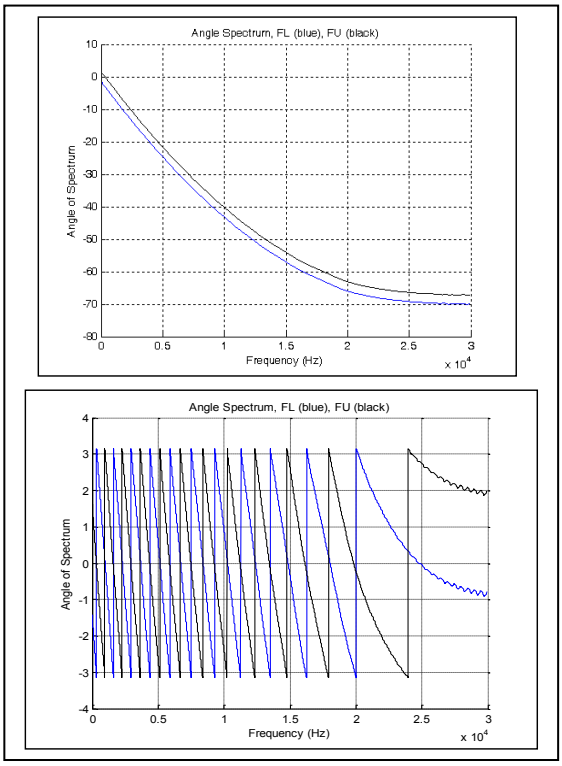

Figure 7. Simulated Differential Phase Spectrum
(Upper Plot: Absolute Phase, Lower Plot: ± π Phase Wrapped)

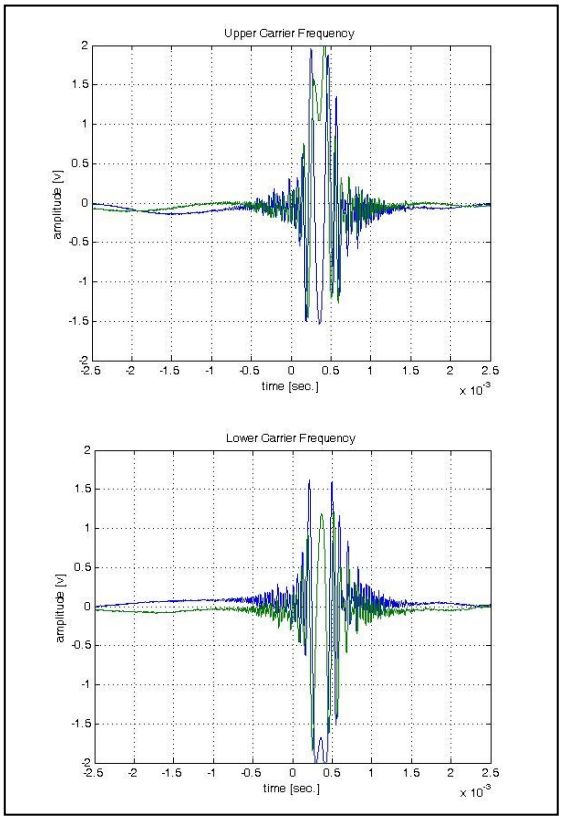

Figure 8. Captured I & Q Data from 7.62mm round at 823 m/s
(Upper Plot: f_U, Lower Plot: f_L)

However, if the actual placement of the shot misses the target centre in both the x and y axes then the declared result has both x and y -axis errors. The summary of errors derived from a parametric study is provided in Table 2 for an assumed baseline between the radars of 2m.

It is worth noting that the error in the declared y –axis result is always negative, i.e. the declared result is always slightly lower than the true miss distance. This arises due to the fact that the measured ranges are slightly too short and so the point of overlap between the two circles of equal range is always closer to the baseline. The sign in the error in the declared x – axis result follows the sign of the true miss distance in the x – axis.

TABLE II. TRAJECTORY INDUCED ERRORS

Trajectory Gradient [radians]	**True Fall of Shot (x,y) [m]**		**Declared Result (x,y) [m]**		**Errors in Declared Result (x,y) [mm]**	
0.08	0	0	0	0.0064	0	-6.4
0.08	0.2	0	0.1987	0.0063	1.3	-6.3
0.08	0	0.2	0	0.2066	0	-6.6
0.08	0.2	0.2	0.1987	0.2064	1.3	-6.4
0.08	-0.2	-0.2	-0.1987	-0.1936	-1.3	-6.4
0.08	0.5	0	0.4968	0.0056	3.2	-5.6
0.08	0	0.5	0	0.5081	0	-8.1
0.08	0.5	0.5	0.4968	0.5064	3.2	-6.4
0.08	-0.5	-0.5	-0.4968	-0.4936	-3.2	-6.4

The results in Table II above represent extreme cases of trajectory gradient and miss distances and yet even so the error in the declared result is typically in the order of 6mm which is nominally the same as the bullet calibre.

TABLE III. MONTE-CARLO ACCURACY SIMULATION RESULTS

SNR [dB]	Δx	σ_x	Δy	σ_y	**CEP**	**Prec**	**Acc**
20	0.37 mm	31.8 mm	0.46 mm	42.4 mm	41.9 mm	53.0 mm	0.62 mm
30	0.09 mm	8.65 mm	0.59 mm	13.6 mm	13.1 mm	16.1 mm	0.61 mm
40	7.6μm	2.52 mm	0.34 mm	4.44 mm	4.04 mm	4.76 mm	0.50 mm
50	24μm	0.75 mm	0.30 mm	1.36 mm	1.27 mm	1.47 mm	0.31 mm

A Monte Carlo study of the effects of noise has also been undertaken and the results presented in Table III. 1000 simulations were conducted adding Gaussian white noise to the baseband signals to give a range of SNR values and assuming a bullet trajectory which has no gradient, i.e. parallel to the z – axis, and passing through the true target centre. This trajectory eliminates other potential sources of error so that the effects of noise alone and processing method can be studied. Table III shows for a range of signal to noise ratios, the mean error in the horizontal axis (Δx), the standard deviation of horizontal errors (σ_x), the mean and standard deviation of errors in the vertical axis (Δy and σ_y), the 50% Circular Error Probable (radius about aim point that contains 50% of reported shots), Precision (standard deviation of cluster of all reports, relative to the cluster mean) and Accuracy (mean of the cluster of reports). The results show that the deviation in the horizontal axis tends to zero as expected, but the Δy and Accuracy results show that there is a 0.3mm upward offset; the offset is due to the mean of the 11 readings that straddle the zero Doppler point being used to reduce noise in the calculation of the radii from each of the radars. The offset can be removed in calibration, or alternative processing methods employed. The Precision and 50% CEP results show clearly that at 40dB or better, the system can measure within a half calibre. Earlier calculations and estimated losses (section IIIB) and measured data (section IVB) suggest that noise-limited detections giving a SNR of about 37 dB are achievable and therefore the unit is capable of sufficient accuracy and precision.

V. CONCLUSIONS

A prototype virtual targeting radar has been designed and built. A system of two radars with orthogonal views each using a dual tone CW waveform forms a very practical solution as an automated virtual target for small arms fire training. The analysis of the radar configuration have been derived which give an x,y targeting function and allow its accuracy to be quantified. The frequency-domain signal processing algorithm has been developed. The prototype provides an exact indication of the miss distance with millimetre-level accuracy. The processing does however assume a trajectory normal to the targeting plane and this assumption introduces maximum errors in the order of bullet calibre. In spite of the simplicity of the design, the hardware costs for bespoke radars has been high.

Future work is planned to use an array of commercially available low-cost radar modules, each of which emit a single CW tone. The signal processing would be extended to account for any arbitrary trajectory gradients. These modifications pave the way for the system to be scaled up to meet the targeting requirements for artillery and tank firing ranges.

REFERENCES

[1] P. Kisatsky, “Determining the position and trajectory of supersonic projectiles from acoustic measurements”, Technical Report ADA392161 (Army Armemant Research Development and Engineering Center Picattiny Arsenal NJ), 2000.

[2] G. Dingley, C. M. Alabaster, “Radar based automatic target system”, IEEE 4th International Conference on Waveform Diversity and Design, Orlando, FL, USA, 8th – 13th February 2009

[3] G. Dingley, “Automatic target system for small arms fire”, M.Phil to PhD transfer thesis, Cranfield University, Shrivenham, UK, August 2008.

[4] J. O’Rourke, Computational geometry in C. Cambridge University press, 1995, pp.306-307.